

Surface-Enhanced Raman Scattering from Intracellular and Extracellular Bacterial Locations

Roger M. Jarvis,[†] Nicholas Law,[‡] Iqbal T. Shadi,[†] Paul O'Brien,[§] Jonathan R. Lloyd,[‡] and Royston Goodacre^{*†}

School of Chemistry, University of Manchester, Manchester Interdisciplinary Biocentre, 131 Princess Street, Manchester M1 7DN UK, School of Earth, Atmospheric and Environmental Sciences, University of Manchester, Manchester M13 9PL UK, and School of Chemistry, University of Manchester, Brunswick Street, Manchester M13 9PL UK

While surface-enhanced Raman scattering (SERS) can increase the Raman cross-section by 4–6 orders of magnitude, for SERS to be effective it is necessary for the analyte to be either chemically bonded or within close proximity to the metal surface used. Therefore most studies investigating the biochemical constituents of microorganisms have introduced an external supply of gold or silver nanoparticles. As a consequence, the study of bacteria by SERS has to date been focused almost exclusively on the extracellular analysis of the Gram-negative outer cell membrane. Bacterial cells typically measure as little as 0.5 by 1 μm , and it is difficult to introduce a nanometer sized colloidal metal particle into this tiny environment. However, dissimilatory metal-reducing bacteria, including *Shewanella* and *Geobacter* species, can reduce a wide range of high valence metal ions, often within the cell, and for Ag(I) and Au(III) this can result in the formation of colloidal zero-valent particles. Here we report, for the first time, SERS of the bacterium *Geobacter sulfurreducens* facilitated by colloidal gold particles precipitated within the cell. In addition, we show SERS from the same organism following reduction of ionic silver, which results in colloidal silver depositions on the cell surface.

Raman spectroscopy is a quantitative vibrational spectroscopic method that can be used to infer structural molecular information or composition from a sample. In Stokes Raman scattering, an exchange of energy occurs between the incident photons and molecules in the lowest vibrational energy level of the molecular ground state, giving rise to scattered photons at wavelengths lower than that of the excitation radiation.¹ Unlike the complementary method of infrared absorbance spectroscopy, which has very broad peak cross-sections, band widths across a Raman spectrum are much narrower and generally in the region of 10–30 cm^{-1} . Therefore, Raman spectroscopy provides a more detailed picture of chemical components in a complex sample and for pure

compounds a greater degree of structural information. The major drawback to the method, however, is the very low efficiency of Stokes Raman scattering, where typically only 1 in 10^6 – 10^8 incident photons are estimated to be scattered inelastically. While this problem is overcome largely through the use of laser light sources, confocal Raman microscopes, and sensitive charge coupled detectors (CCDs),^{2,3} there can often be problems with analyzing complex biological samples which tend to exhibit broad fluorescence backgrounds under visible and near-infrared (NIR) excitation.⁴

Consequently, researchers have been investigating enhanced Raman methods as a means of overcoming the shortcomings of conventional visible/NIR Raman spectroscopy. One approach is to use deep ultraviolet excitation, where incident wavelengths with energies close to the molecular electronic transitions of certain chromophores result in a larger Raman cross-section for an experiment, a process known as ultraviolet resonance Raman (UVR) enhancement.⁵ An additional benefit is that fluorescence is often shifted beyond the observed spectral range,⁶ although a major drawback is that photochemical damage (due to the absorbing centers giving rise to the resonance enhanced Raman bands) needs to be avoided by using often burdensome sample presentation methods.^{7,8}

An alternative and more sensitive method of increasing the Raman cross-section is to use surface-enhanced Raman scattering (SERS^{9,10}). This technique makes use of a roughened metal surface, often colloidal particles, which upon illumination with a light source gives rise to surface plasmon oscillations that produce an enhanced local optical field (so-called electromagnetic enhancement), thus increasing the Raman cross-section by very large (up

* Author to whom correspondence should be addressed. E-mail: Roger.Jarvis@manchester.ac.uk. Phone: +44 161 3065145. Fax: +44 161 3064519.

[†] School of Chemistry.

[‡] School of Earth, Atmospheric and Environmental Sciences.

[§] School of Chemistry.

(1) Banwell, C. N. *Fundamentals of Molecular Spectroscopy*, 3rd ed.; McGraw-Hill: Maidenhead, U.K., 1983.

(2) Williams, K. P. J.; Pitt, G. D.; Batchelder, D. N.; Kip, B. J. *Appl. Spectrosc.* **1994**, *48*, 232–235.

(3) Williams, K. P. J.; Pitt, G. D.; Smith, B. J. E.; Whitley, A.; Batchelder, D. N.; Hayward, I. P. *J. Raman Spectrosc.* **1994**, *25*, 131–138.

(4) Goodacre, R.; Timmins, E. M.; Burton, R.; Kaderbhai, N.; Woodward, A.; Kell, D. B.; Rooney, P. J. *Microbiology* **1998**, *144*, 1157–1170.

(5) Spiro, T. *Trends Biochem. Sci.* **1976**, *1*, 109.

(6) Spiro, T. G. *Acc. Chem. Res.* **1974**, *7*, 339–344.

(7) Chen, X. G.; Lemmon, D. H.; Bormett, R. W.; Asher, S. A. *Appl. Spectrosc.* **1992**, *47*, 248–249.

(8) Lopez-Diez, E. C.; Goodacre, R. *Anal. Chem.* **2004**, *76*, 585–591.

(9) Fleischmann, M.; Hendra, P. J.; McQuillan, A. J. *Chem. Phys. Lett.* **1974**, *26*, 163–166.

(10) Jeanmaire, D. L.; Vanduyne, R. P. *J. Electroanal. Chem.* **1977**, *84*, 1–20.

to 10¹⁴) factors.¹¹ The mechanism is still not understood fully, and a charge-transfer effect known as chemical enhancement is also thought to contribute to the overall enhancement effect of SERS.¹² An additional augmentation of the signal can result from a resonance enhancement effect in surface-enhanced experiments for absorbing species at the incident wavelength; this effect is described as surface-enhanced resonance Raman scattering (SERRS^{13–15}).

SERS has now been applied widely to the study of bacterial cells,^{16–23} for a recent review article on bacterial SERS research, see ref 24. Initial investigations sought to obtain representative SERS spectral fingerprints of typical laboratory strains;²² later the method was shown to be sufficiently reproducible to distinguish between bacterial cells isolated from patients with urinary tract infections to the subspecies level.¹⁶ More recent work has demonstrated further categorical modeling applications of SERS for other bacterial genera and the investigation on limits of detection in terms of the amount of biomass required to obtain SERS spectra of bacteria.¹⁹ In addition, many of these studies have been carried out using a range of incident wavelengths with a variety of colloidal metal preparations. To date, no standard approach has been developed and this may be due to problems associated with the reproducibility of SERS, which could be ascribed to many possible experimental factors, including colloidal particle morphology, geometric considerations with respect to the analyte–metal interface, saturation of the particle surface, and spatial localization of the SERS active substrate. So far, SERS has been used to probe only the surface of bacterial cells, due to the difficulty associated with introducing nanometer sized metal particles into such small structures (typically 0.5 μm by 1 μm). While one article claims to demonstrate SERS from internalized colloids,²⁵ no actual SERS spectra under these conditions were reported.

It is known that certain Fe(III)- and sulfate-reducing bacteria can form (colloidal) metal particles through electron transfer to gold and silver ions.²⁶ These microorganisms include species from the genera *Geobacter* and *Shewanella* and have been studied widely, due to their potential use in many environmental and biotechnological processes including the bioremediation of metal

and radionuclide contaminated land and water, the oxidation of xenobiotics under anaerobic conditions, metal recovery, and the formation of novel biocatalysts (reviewed in ref 27). Recently Biju and colleagues²⁸ reported SERS with 514.5 nm excitation on *Shewanella oneidensis* with extracellular enhancement enabled by a silver coated slide and did not investigate the potential ability of this organism to reduce Ag(I).

In this study, we report SERS of *Geobacter sulfurreducens* using an alternative and highly novel approach, using colloidal metal substrates prepared from the enzymatic reduction of silver and gold salts by these bacteria. In the case of exposure to Ag(I), transmission electron micrographs of whole and sectioned cells show extracellular colloidal silver precipitation. By contrast, when Au(III) is reduced the colloidal depositions are shown to reside almost exclusively within the cytoplasm close to the inner cell membrane. We believe that this is the first conclusive report of SERS from the internal structure of a bacterial cell.

MATERIALS AND METHODS

Preparation of Bacterial Cultures. *Cultivation Conditions.* *G. sulfurreducens* (ATCC 51573) was obtained from DSMZ and grown under strictly anaerobic conditions at 30 °C in modified fresh water medium in serum bottles sealed with butyl rubber stoppers, as described previously.²⁹ Sodium acetate (25 mM) and fumarate (40 mM) were provided as the electron donor and acceptor, respectively. All manipulations were done under an atmosphere of N₂/CO₂ (80:20). Cells grown to midlog phase were harvested by centrifugation (4075g for 20 min) and washed three times with 30 mM sodium bicarbonate buffer (pH 7.0) equilibrated with N₂/CO₂ (80:20) prior to use. Cells were then exposed to 200 μM Ag(I) or Au(III) as AgNO₃ and HAuCl₄·3H₂O, respectively, dissolved in 30 mM bicarbonate buffer. Acetate (10 mM) was added as the electron donor for silver reduction, and hydrogen (bubbled through the solution for 5 min) was used for gold reduction.²⁹

Raman Spectroscopy and SERS. Raman and SERS spectra were recorded on a Renishaw (Renishaw plc., Old Town, Wotton-under-Edge, Gloucestershire, U.K.) System 2000 confocal Raman microscope,^{2,3} with a resolution of ~6.5 cm⁻¹. For cells exposed to Ag(I), a 20 mW 633 nm HeNe laser source was used yielding ~2 mW power at the sample. Spectra of cells exposed to Au(III) were acquired using a high-power (300 mW) 830 nm NIR diode laser source, with power at the sampling point ~30 mW. Control spectra of cells that had not been exposed to metal salts were obtained at each respective wavelength, and in every case Raman and SERS spectra were acquired over a Stokes Raman shift of 200–2000 cm⁻¹ with 60 s integration.

Transmission Electron Microscopy. Transmission electron microscopy (TEM) was used to identify the cellular location of the metal particle products of Ag(I) and Au(III) reduction. Cells were collected by centrifugation under nitrogen and washed three times in anaerobic 100 mM HEPES buffer (pH = 7), then fixed with 2.5% glutaraldehyde overnight. Cells were then washed with HEPES buffer and enrobed in 2% noble agar. Agar blocks were processed through a gradual ethanol dehydration sequence (25,

- (11) Nie, S. M.; Emery, S. R. *Science* **1997**, *275*, 1102–1106.
- (12) Otto, A.; Mrozek, I.; Grabhorn, H.; Akemann, W. *J. Phys.: Condens. Matter* **1992**, *4*, 1143–1212.
- (13) Graham, D.; Mallinder, B. J.; Whitcombe, D.; Smith, W. E. *Chem. Phys. Phys. Chem.* **2001**, *12*, 746–748.
- (14) Graham, D.; Mallinder, B. J.; Whitcombe, D.; Watson, N. D.; Smith, W. E. *Anal. Chem.* **2002**, *74*, 1069–1075.
- (15) Graham, D.; Smith, W. E.; Linacre, A. M. T.; Munro, C. H.; Watson, N. D.; White, P. C. *Anal. Chem.* **1997**, *69*, 4703–4707.
- (16) Jarvis, R. M.; Goodacre, R. *Anal. Chem.* **2004**, *76*, 40–47.
- (17) Jarvis, R. M.; Goodacre, R. *Anal. Chem.* **2004**, *76*, 5198–5202.
- (18) Premasiri, W.; Moir, D.; Klempner, M.; Krieger, N.; Jones, G.; Ziegler, L. *J. Phys. Chem. B* **2005**, *109*, 312–320.
- (19) Sengupta, A.; Mujacic, M.; Davis, E. J. *Anal. Bioanal. Chem.* **2006**, *386*, 1379–1386.
- (20) Jarvis, R.; Clarke, S.; Goodacre, R. *Topics Appl. Phys.* **2006**, *103*, 397–408.
- (21) Jarvis, R. M.; Brooker, A.; Goodacre, R. *Faraday Discuss.* **2006**, *132*, 281–292.
- (22) Zeiri, L.; Bronk, B. V.; Shabtai, Y.; Czege, J.; Efrima, S. *Colloids Surf., A* **2002**, *208*, 357–362.
- (23) Zeiri, L.; Bronk, B. V.; Shabtai, Y.; Eichler, J.; Efrima, S. *Appl. Spectrosc.* **2004**, *58*, 33–40.
- (24) Jarvis, R.; Goodacre, R. *Chem. Soc. Rev.* **2008**, DOI: 10.1039/b705973f.
- (25) Efrima, S.; Bronk, B. V. *J. Phys. Chem. B* **1998**, *102*, 5947–5950.
- (26) Lloyd, J. R. *FEMS Microbiol. Rev.* **2003**, *27*, 411–425.

- (27) Lloyd, J.; Lovley, D.; Macaskie, L. *Adv. Appl. Microbiol.* **2004**, *53*, 85–128.
- (28) Biju, V.; Pan, D.; Gorby, Y. A.; Fredrickson, J.; McLean, J.; Saffarini, D.; Lu, H. P. *Langmuir* **2007**, *23*, 1333–1338.
- (29) Lloyd, J.; Leang, C.; Myerson, A. H.; Coppi, M.; Cuifio, S.; Methe, B.; Sandler, S.; Lovley, D. *Biochem. J.* **2003**, *369*, 153–161.

50, 75, 95% ethanol in deionized water), and three 15 min washes in 100% ethanol. The specimens were embedded in LR white resin (London Resin Company, Theale, Berkshire, U.K.). Increasing concentrations of LR white resin in ethanol were infiltrated into the agar block with one 15 min wash in an LR white: ethanol (50:50) mixture, followed by two 2 h 100% LR white steps. The agar blocks were then cured for 24 h at 60 °C. Ultrathin sections of 60–80 nm thickness were sectioned from the embedded blocks using a microtome and mounted on Formvar and carbon coated copper TEM grids. Sections were stained with 2% uranyl acetate in distilled water for 5 min and lead staining solution for 5 min prior to TEM analysis. Samples were first examined using a FEI Tecnai 12 Biotwin transmission electron microscope (FEI, Eindhoven, The Netherlands) at 100 kV, then they were transferred to FEI Tecnai F30 operating at 300 kV (FEI, Eindhoven, The Netherlands) coupled with a high-angle annular dark field detector for EDX analysis.

X-ray Diffraction. X-ray diffraction (XRD) measurements from resting cells exposed to either Ag(I) or Au(III) were obtained using a Bruker D8 Advance X-ray diffractometer (Bruker AXS Ltd., Coventry, U.K.). Cells with precipitate were washed using anaerobic water; these were then dried under air and ground to very fine powder and mixed with amyl acetate to form a uniform film on a glass slide, which was transferred immediately to the instrument. The step size used was 0.02°, and the scan time was 5–10 s. During sample preparation, illumination with direct light was avoided.

RESULTS AND DISCUSSION

Extracellular Colloidal Silver SERS. *G. sulfurreducens*³⁰ and related species have been the focus of much recent interest due to their ability to couple the oxidation of organic matter in the subsurface to the reduction of a wide range of high valence metals. These include poorly soluble Fe(III) oxides, the normal physiological substrate for these anaerobic bacteria in anoxic aquifer sediments, and also contaminant metals and radionuclides such as soluble Cr(VI) and U(VI), which can be precipitated through bioreduction.³¹ The reduction and precipitation of precious metals such as Au(III) and Ag(I) has received less attention, although such processes could be used to recover gold and silver from dilute solutions and could also be used *in vivo* to generate nanoscale colloidal gold and silver precipitates to obtain SERS data.

Late log phase cultures of *G. sulfurreducens* were challenged with Ag¹⁺ ions (with acetate as the electron donor) and assessed for the production of elemental silver particle formation through X-ray diffraction analysis, TEM imaging, and energy dispersive X-ray (EDX) spectroscopy. XRD analysis confirmed the formation of elemental silver in these experiments (Figure 1C), while TEM analysis showed whole cells of *G. sulfurreducens* surrounded by an array of electron dense colloidal silver particles across and around the cell surface (parts A and B of Figure 1). EDX (Figure 1D) confirmed that these nanoparticles contain a high level of silver, and the silicon peaks observed are probably from contact with glass. In addition to acetate, hydrogen was also tested as an

electron donor but did not support efficient reduction of Ag(I) to Ag(0). The silver particles produced with acetate as the electron donor were small, ~30 nm across, exhibited a fairly homogeneous size distribution, and were monodispersed across the cell sample; although due to their very small size, it was difficult to establish morphology with any certainty. Figure 1B shows cells from the same culture in cross section, confirming an extracellular location for the precipitated silver; four colloidal particles can be seen clearly outside the cell.

Cells from this same culture were also analyzed using Raman microspectroscopy, for which SERS was observed (Figure 2), along with cells from a control culture that had not been exposed to Ag(I). In both cases, incident radiation at a 633 nm wavelength was used, which we observed to give good SERS using silver colloid. Typical Raman and SERS spectra for the control and SERS active samples are shown in Figure 2, with tentative band assignments summarized in Table 1. With comparison of the conventional Raman spectrum against its SERS counterpart, there are negligible bands that complement one another across the two spectra, which is to be expected given the difference in selectivity that is imposed through the SERS process. Two peaks stand out in the SERS spectrum as potential resonance enhanced bands, at 924 and 1061 cm⁻¹, although so far we are unable to provide accurate assignments for these. Also notable are the amide III (~1247 cm⁻¹) and amide I (~1562 cm⁻¹) peaks, present on both the control (Raman) and SERS spectra, which exhibit quite different profiles. The amide I and III band symmetry is known to provide an insight into protein backbone structure;^{32,33} however, it is difficult to understand in this context what structural information could be inferred from the analysis of such a complex sample. The sharper peaks in these regions of the SERS spectrum could suggest a significant chemical enhancement effect¹² with respect to protein complexes.

Most of the additional characterized features on the SERS spectrum point to aliphatic vibrations (Table 1), although there is a potential contribution from phenylalanine at 625 cm⁻¹. Clearly, the lack of a comprehensive database of SERS band assignments makes the process of annotating the spectra less valuable than it would be otherwise. Although, given the density of peaks in the SERS spectrum, there is great potential for obtaining biologically interesting information once such a resource becomes available.

Intracellular Colloidal Gold SERS. The ability of certain organisms to precipitate gold by reduction from solution at both extra- and intracellular sites has been noted previously.^{34,35} It is apparent from these studies that the electron donor provided in the culture medium is very important in determining the organism's ability to reduce certain ionic metals, although the mechanism for intra- versus extracellular reduction is not understood.

In contrast to the results for silver, gold was reduced with hydrogen rather than acetate as an electron donor by *G. sulfurreducens*, and the cells exposed to ionic gold did not differ morphologically from those exposed to ionic silver. From parts A

(30) Caccavo, F.; Lonergan, D. J.; Lovley, D. R.; Davis, M.; Stolz, J. F.; McInerney, M. J. *Appl. Environ. Microbiol.* **1994**, *60*, 3752–3759.

(31) Lloyd, J. *FEMS Microbiol. Rev.* **2003**, *27*, 411–425.

(32) Taylor, K.; Cheng, N.; Williams, R.; Steven, A.; Wickner, R. *Science* **1999**, *283*, 1339.

(33) Vogel, H.; Jahng, F. J. *Mol. Biol.* **1986**, *190*, 191–199.

(34) Kashefi, K.; Tor, J. M.; Nevin, K. P.; Lovley, D. R. *Appl. Environ. Microbiol.* **2001**, *67*, 3275–3279.

(35) Konishi, Y.; Tsukiyama, T.; Ohno, K.; Saitoh, N.; Nomura, T.; Nagamine, S. *Hydrometallurgy* **2006**, *81*, 24–29.

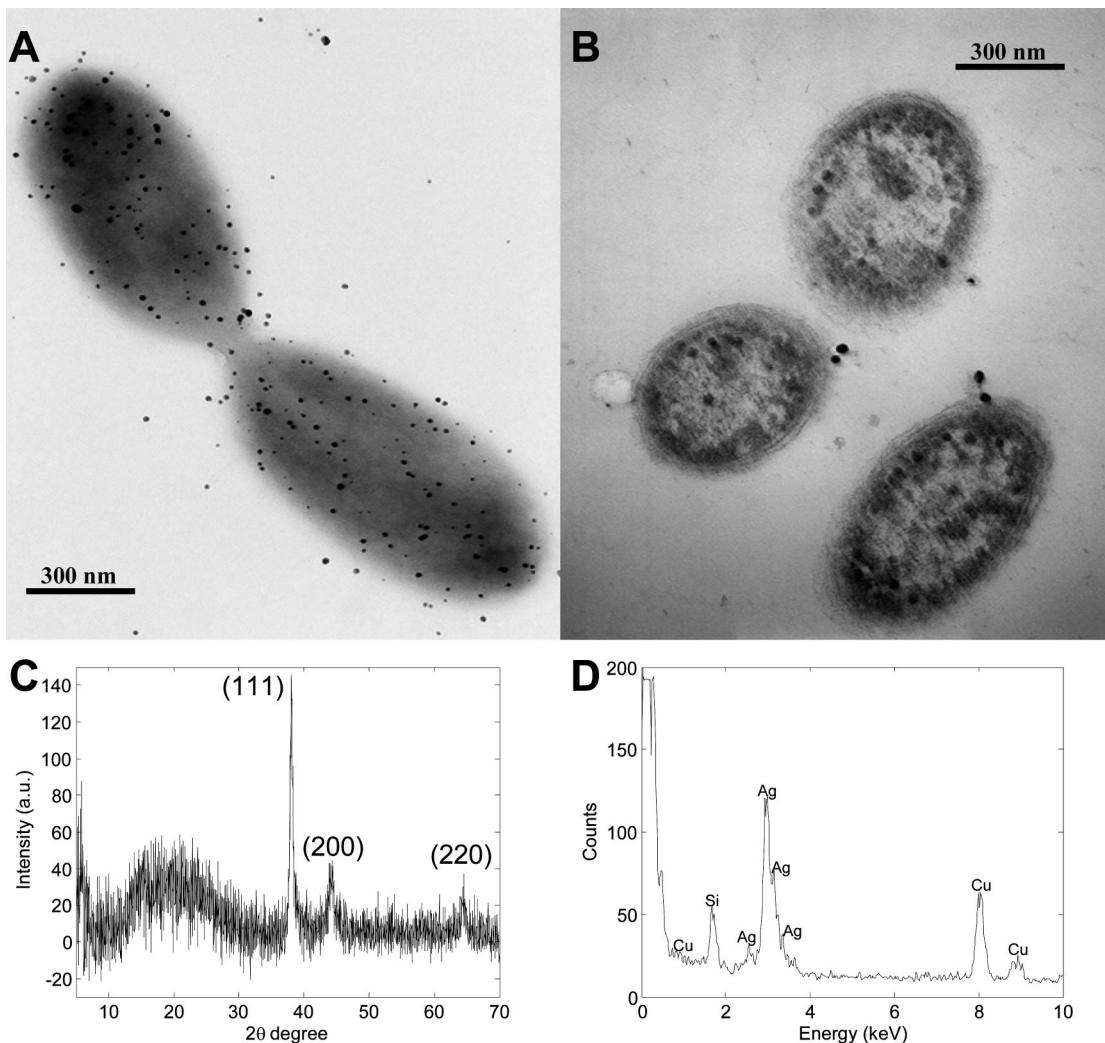


Figure 1. TEM images of *G. sulfurreducens* with colloidal silver deposits, (A) image showing whole cells; (B) cross section through cells. (C) XRD profile acquired from resting *G. sulfurreducens* cells exposed to 200 μM Ag(I). (D) EDX profile acquired from the same cells.

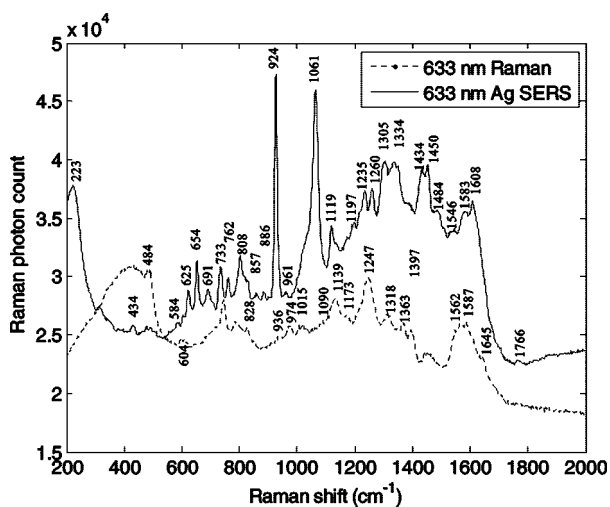


Figure 2. Raman (dotted line) and SERS (solid line) spectra of *G. sulfurreducens* acquired using 633 nm excitation, with the latter in the presence of a colloidal silver substrate. Also highlighted are the main bands observed.

and B of Figure 3, it is clear that *G. sulfurreducens* reduces Au(III) and precipitates Au(0) and that under these conditions the resultant colloidal gold particles are clearly positioned within the

Table 1. Tentative Band Assignments for SERS Spectra Acquired from *G. sulfurreducens* with Extracellular Colloidal Silver at 633 nm Excitation^{38–41}

Raman shift (cm^{-1})		tentative assignment ^a
Raman	SERS	
	625	Phe (skeletal)
	733	$\rho(\text{CH}_2)$
746		Tyr (ring breathing)
828		$\nu(\text{CON})$ symmetric; $\delta(\text{CCH})$ aliphatic
	857	$\nu(\text{CC})$ $\nu(\text{COC})$ 1,4-glycosidic link
	924	unassigned
936		(νCOC), CO dominated ring vibrations of carbohydrates, (νCOP), (νPOP)
	1061	unassigned
1235–1260	1235–1260	amide III
	1334	$\delta(\text{CH})$
1397		$\nu(\text{CO})$ symmetric COO^-
1430–1455	1430–1455	$\delta(\text{CH}_2)$ (saturated lipids)
1546–1645	1546–1645	$\delta(\text{NH})$ & $\nu(\text{CN})$, amide II

^a δ , Deformation; ν , stretching; ρ , rocking; Phe, phenylalanine; Tyr, tyrosine.

cell. This is further confirmed by EDX spectroscopy (Figure 3D) and a purple colored product (data not shown), consistent with colloidal gold and the XRD trace obtained from these cells (Figure

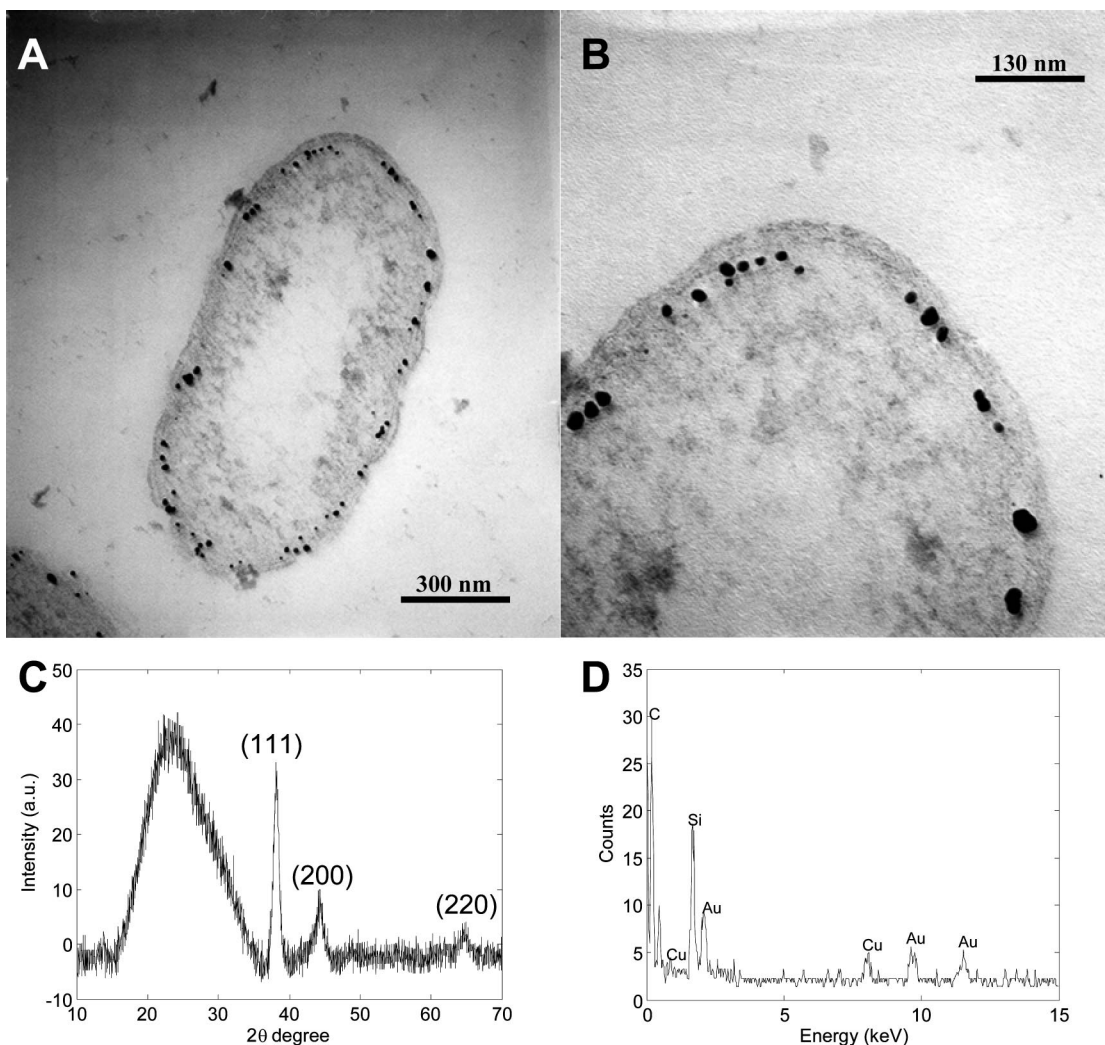


Figure 3. TEM images of *G. sulfurreducens* with colloidal gold deposits, (A) low magnification cell cross section; (B) high magnification cell cross section. (C) XRD profile acquired from resting *G. sulfurreducens* cells exposed to 200 μM Au(III). (D) EDX profile acquired from the same cells.

3C). The individual gold particles synthesized from the in vivo reduction of Au(III) were similar in size with the silver particles (~ 30 nm) and are highly monodisperse within the cell. From our TEM analyses (parts A and B of Figure 3), the site of precipitation seems to be in the cytoplasm along the inner cellular membrane. The monodispersed nature of the Au (and indeed Ag) particles will most likely mean that a maximum SERS enhancement is not being achieved, as studies have shown the importance of colloidal aggregation to maximize the Raman cross section for SERS.³⁶

Once again, a comparison of a control Raman spectrum of the *Geobacter* cells was made against a SERS spectrum acquired from an aliquot of the same gold inoculated culture from which the XRD results and TEM images were obtained (Figure 4). This time the excitation wavelength used was at 830 nm, principally because SERS was not observed at 633 nm for gold and colloidal gold SERS has been shown to be effective at this wavelength previously.³⁷ Likewise, SERS was not observed for the cells exposed to silver

at 830 nm, preventing direct comparisons between the colloidal gold and silver SERS spectra at both incident frequencies.

The Raman spectrum of *G. sulfurreducens* in Figure 4 is markedly different to that acquired at 633 nm (Figure 2), very little chemical information is present with only two distinct bands at 1032 and 1069 cm^{-1} . Similar amounts of material were used in each case, with an excess of biomass predicted to be present within the collection volume. Despite equivalent integration times for all spectra and greater power at the sampling point with the 830 nm diode laser, the total scattering cross section is approximately one-fifth of that observed for both Raman and SERS (with colloidal silver) at 633 nm. Of course, despite the low power red source used, at shorter wavelengths the Raman cross-section benefits from a ν^4 increase in intensity; however, that would not in itself account for the large differences observed.

(36) Moskovits, M.; Tay, L. L.; Yang, J.; Haslett, T. In *Optical Properties of Nanostructured Random Media*; Springer: New York, 2002; Vol. 82, 215–226.

(37) Kneipp, K.; Haka, A. S.; Kneipp, H.; Badizadegan, K.; Yoshizawa, N.; Boone, C.; Shafer-Peltier, K. E.; Motz, J. T.; Dasari, R. R.; Feld, M. S. *Appl. Spectrosc.* **2002**, *56*, 150–154.

(38) Britton, K. A.; Dalterio, R. A.; Nelson, W. H.; Britt, D.; Sperry, J. F. *Appl. Spectrosc.* **1988**, *42*, 782–788.

(39) Edwards, H. G. M.; Russell, N. C.; Weinstein, R.; Wynnwilliams, D. D. *J. Raman Spectrosc.* **1995**, *26*, 911–916.

(40) Lin-Vien, D.; Colthup, N.; Fateley, W.; Grasselli, J. *The Handbook of Infrared and Raman Characteristic Frequencies of Organic Molecules*; Academic Press: New York, 1991.

(41) Williams, A. C.; Edwards, H. G. M. *J. Raman Spectrosc.* **1994**, *25*, 673–677.

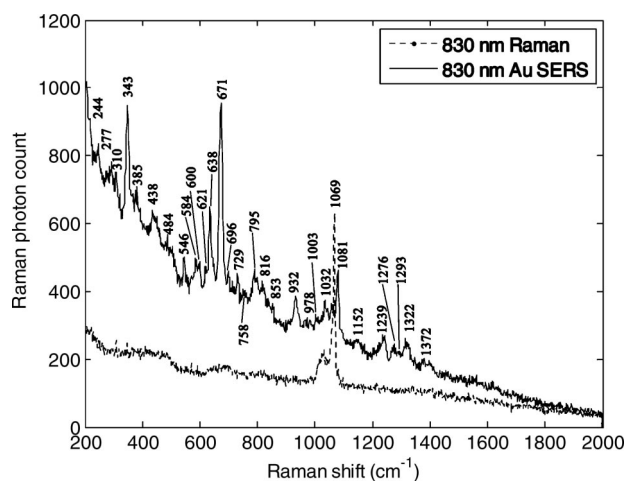


Figure 4. Raman (dotted line) and SERS (solid line) spectra of *G. sulfurreducens* acquired using 830 nm excitation, with the latter in the presence of a colloidal gold substrate. Also highlighted are the main bands observed.

Comparison of SERS at each wavelength in the presence of different metal substrates, not unsurprisingly, shows very large differences. Most distinctively there is an absence of the amide I peak in the SERS spectrum under gold conditions, with some information present in the amide III region at $\sim 1250\text{ cm}^{-1}$. This latter observation is perhaps encouraging since neither the amide I nor III peaks occur in the Raman spectrum at 830 nm, and SERS is therefore providing enhancement of key protein related features in the spectrum, which are likely to be membrane associated proteins in the inner membrane of this Gram-negative microorganism, as well as cytosolic proteins.

Given the intracellular location of the gold particles and the highly local enhancement effect of SERS (in the order of a few Å), the SERS spectrum in Figure 4 is likely to contain biochemical components unique to the bacterial intracellular space. It is therefore encouraging to note that several bands corresponding to nucleic acids could be tentatively assigned (Table 2), which were absent from extracellular information afforded by the SERS spectrum from silver particles (Figure 2). Once again, one must be cautious in reporting the provenance of these peaks and this situation will improve once more spectra are acquired from complex systems and their individual components, a task in which we are currently engaged.

CONCLUSIONS

Geobacter spp. are well-known to have abundant *c*-type cytochromes that provide an electron chain to the outside of the cell for the reduction of extracellular electron acceptors such as poorly soluble Fe(III) oxides; therefore, it was not surprising to note the extracellular reduction and precipitation of silver. However, the ability to constrain the precipitation of gold nanoparticles to the compartments within the cell was unexpected, and the exact

Table 2. Tentative Band Assignments for SERS Spectra Acquired from *G. sulfurreducens* with Intracellular Colloidal Gold at 830 nm Excitation^{38–41}

Raman shift (cm^{-1})		
Raman	SERS	tentative assignment ^a
	546	CO, POC bending (phospholipids, nucleic acids)
	671	$\nu(\text{CS})$
	729	$\rho(\text{CH}_2)$
	795	$\nu(\text{PO}_2)$, $\nu(\text{CC})$ ring breathing (RNA/DNA)
	816	COPOC in A-RNA backbone
	853	$\nu(\text{CC})$ $\nu(\text{COC})$ 1,4-glycosidic link
	1003	$\nu(\text{CC})$ aromatic ring (Phe)
1032		unassigned
1069		unassigned
	1081	$\nu(\text{PO})$ (symmetric) of PO_2^- ; $\nu(\text{COC})$ aliphatic esters, oligonucleotides, polysaccharides.
	1239–1293	amide III
	1322	adenine, guanine, Tyr

^a δ , Deformation; ν , stretching; ρ , rocking; Phe, phenylalanine; Tyr, tyrosine.

biochemical mechanism of reduction is not understood and warrants further investigation.

Currently there is considerable interest in the diverse metabolism of *Geobacter* species and other metal-reducing bacteria which can be harnessed for a wide-range of biotechnological processes. We believe that SERS offers a nontargeted exquisitely sensitive chemical analysis that could be used for a range of fundamental and applied studies.²⁴ For instance, the mechanisms of metal reduction and precipitation, as well as the biotransformation of organic contaminants, need further study and these research areas could be facilitated by SERS, potentially at the resolution of a single cell, as demonstrated in ref 17.

In conclusion, this study reports conclusively for the first time, SERS from the interior of a bacterial cell measuring no more than $0.5\ \mu\text{m} \times 1.5\ \mu\text{m}$. With the use of this approach, there is now clear potential for SERS to be used in a targeted analysis of intracellular compartments as well as surface membrane analysis.

ACKNOWLEDGMENT

R.M.J. and R.G. would like to thank the United Kingdom Home Office for funding. P.O'B., I.T.S., and R.G. are indebted to the EBS committee of the U.K. BBSRC. J.R.L. and N.L. would like to acknowledge financial support from the U.S. DOE ERSP and EPSRC. The authors would also like to thank the staff in the Faculty of Life Sciences Electron Microscope Facility for their assistance and the Wellcome Trust for equipment grant support to the EM Facility.

Received for review April 25, 2008. Accepted June 30, 2008.

AC800838V